Sunan Kalijaga of Journal Physics
Vol. 5, No. 2, 2023, pp. 51 - 62
ISSN: 2715-0402, DOI:

Estimating the weight of Ongole crossbreed cattle based on image data using CNN and linear regression methods

Gumelar Syahrul[1*], Anggraini Eca[2]
[1] RnD Division, PT Griya Kreasi Teknologi, Jl. Pertamina 17610, Indonesia
[2] Sensing Technology, Defense University, Jl. Salemba Raya 10440, Indonesia
* Corresponding Author

ARTICLE INFO

Article history:

Received January 15, 2023
Revised February 18, 2023
Accepted Maret 20, 2023

Keywords:

CNN;
Image processing;
Linear regression;
Ongole cow;
Weight estimation

ABSTRACT

One of contributors to food needs, especially meat, is Ongole crossbreed cow, commonly known as PO cattle. In these livestock activities, necessary to monitor the weight of the cows with the aim of assessing the selling price of cattle and monitor health condition of the cows. Currently, farmers still use traditional methods such as manual forecasts or scales in measuring the weight of cows. Therefore, in this study we explore using camera as an alternative instrument for measuring cow weight. The research stages include image data acquisition, preprocessing, cow body segmentation, weight estimation and system evaluation. The image data acquisition process obtained with DSLR camera device. Preprocessing using a kernel sharpening filter. Cow body segmentation using the Mask R-CNN method. The cow body image then processed for weight estimation training using CNN and Linear Regression methods. The results of system evaluation at segmentation stage managed to get the metric value of Intersection over Union (IoU) of 0.86. In weight estimation results, RMSE metric value 1.10, MAE metric value 0.24, MAPE metric value 0.06%, and R2 metric value 0.99.

Cite Article:

Gumelar Syahrul and Anggraini Eca, "Estimating the weight of Ongole crossbreed cattle based on image data using CNN and linear regression methods" Sunan Kalijaga of Journal Physics, vol. 1, no. 1, pp. 51 - 62, 2023, doi: .

1. INTRODUCTION

One of the contributors to food needs, especially meat, is the breeding of Ongole crossbreed cattle or commonly known as PO cattle. The process of calculating the weight of cattle is needed by both breeders and traders to determine the health level of cattle and the selling price of cattle. Calculating the weight of the cow can be done using a special cattle weight scale. However, because of its large dimensions and high price, not all breeders or traders have these scales. So the alternative measurement is usually done manually by cattle breeders or middlemen based on visual eye observations. However, this is very subjective because each person has a different perspective in estimating. Along with technological developments, especially in the field of digital image processing and the methods therein. Digital image processing has been widely studied by previous researchers.

Research on Real-Time Detection Methods in Image Processing - Based Civil Structure Cracks was researched by Luo [1]. Damage Detection of Nomex Sandwich Carbon Face Sheet Composite using Image Processing Techniques was researched by Saritas [2]. Location and Characterization of Harmonic Sources Based on Allowable Current Limits Using Deep Learning and Image Processing was researched by Eslami [3]. Electrical transformer fault diagnosis based on infrared image processing and semi-supervised learning

was researched by Fang [4]. The Application of Digital Image Processing Technology in Finding Green Patches in the Saudi Arabian Desert was researched by Mehdi [5].

Automatic Detection of Corneal Ulcers Using a Combination of Image Processing and Deep Learning was researched by Qasmieh [6]. Bacterial and yeast counts in microbial bioproducts using digital image processing were investigated by Martín [7]. Predictive selection rules of the preferred image processing method for X-ray microcomputed tomography images on tablets were researched by Bollmann [8].

Agricultural Product Quality Inspection Methods Based on Image Processing were researched by Liu [9]. Utilizing deep learning and advanced image processing techniques to investigate the microstructure of waxy asphalt was researched by Hasheminejad [10]. Characterization of a Micro Beam Fabricated with 3D Technology Using Image Processing Algorithm was researched by Ertugrul Ertugrul [11].

Communication–Multimodal Image Correlation in Two-Dimensional Materials via Automatic Image Processing with Strain and Doping Analysis was researched by Schmidt [12]. Establishment of a simple method for evaluating mixing time in plastic bag photobioreactors using image processing based on freeware tools was researched by Wurm [13]. Digital image processing for analysis of the physical basis for predicting electrical failures in XLPE power cables based on field simulations using the finite element method was researched by Talaat [14].

The Initial Stages of COVID-19 Detection Using Image Processing were researched by Alhaj [15]. The Development of an Automatic Tracking Camera System that Integrates Image Processing and Machine Learning was researched by Fujitake [16]. An intelligent water quality monitoring method based on image processing and RVFL-GMDH model was researched by Chen [17].

Experimental Study of Fluidelastic Instability of Tube Bundles With Asymmetric Stiffness Using a Visual Image Processing System was researched by Tan [18]. Feature Extraction and Image Retrieval of Scenery Images Based on Image Processing was researched by Li [19]. Separating background components in an off-axis holographic mirror-based imaging system using spectral image processing was researched by Matsui [20].

Distributed Environment with Rough Set Theory Based Image Processing Approach for Facial Disturbance Analysis for Better Cosmetic Product Recommendation was researched by Prasuna [21].

A multiple relaxation time lattice Boltzmann scheme for the advection diffusion equation with applications to radar image processing was investigated by Michelet [22]. A survey of Segmentation Techniques for Image Processing was researched by Jasim [23]. The application of holography and automatic image processing to laboratory experiments on the mass and falling speed of small cloud ice crystals was investigated by Weitzel [24].

Highly machinable static separation of fresh concrete based on image processing method was researched by Cui [25]. Radar Interferometry and Optical Satellite Image Processing Methods for Studying Negative Impacts on the Environment (Case Study at the Baikalsk Pulp and Paper Mill) were researched by Bondur [26]. Assessment of Iron Deficiency in Soybeans Using Image Processing and Decision Tree Based Models was researched by Hassanijalilian [27].

Real-Time Implementation of a New Automatic Gain Control Algorithm for MPSoC Based Infrared Image Processing was researched by Hung [28]. Fire Detection in Images Using a Framework Based on Image Processing, Motion Detection, and Convolutional Neural Networks was researched by Koklu [29]. Embedded Single Chip Image Processor and Fingerprint Sensor RISC MCU was researched by Jung [30].

The number of methods or algorithms really depends on the case of each research. Several studies related to methods for estimating the weight of cattle using the multiclass SVM classification method, estimating the weight of sheep using the auto-encoder segmentation method and ANN Regression, estimating the weight of pigs using the deep learning back-propagation method and others.

This research designed a cattle weight estimator system based on image data from camera hardware to make it easier for farmers to reduce confusion and errors in the process of calculating cattle weight. The image data of the cow object taken is from the side and then segmented using the Mask R-CNN method, then the CNN method and regression model will be used to estimate the weight of the cow.

2. METHODS

2.1. Materials and Equipment

The material used in this research is digital image data from the side of the cow's body. Image data was obtained from farms at the Kendal Class A Integrated Livestock Cultivation and Breeding Center, Central Java. Parameter limitations for data collection on materials processed in this research are shown in Table 1. The equipment used includes a DSLR camera and tripod, personal computer, cloud computing platform Kaggle Notebook or Google Colab, Python programming language and other programming libraries.

Table 1. Parameter Data retrieval limitations

Parameter	Description or Specifications
Type of Cow	Ongole crossbreed. (P.O.)
Weight Range	250 – 450 kg
Camera Distance to Cow	2 meters
Camera Height	130 cm

2.2. System Design Analysis

In this research, the system was designed to have several stages, namely pre-processing, image segmentation stage, designing a convolutional neural network (CNN) and regression model, calculating the estimated weight of the cow and finally evaluating the weight estimation results obtained. Before entering this stage of the process, this research will carry out two training processes and the formation of mathematical models. The first model is used for the cow image segmentation process using the Mask R-CNN method. Then the second model is used to estimate cow weight using the CNN regression model architecture. The following general process flow diagram is shown in Figure 1.

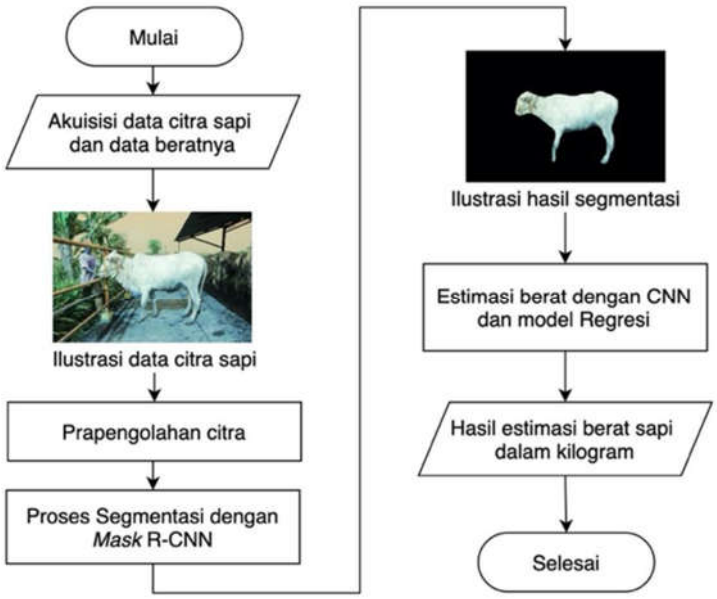

Gambar 1 Diagram alir tahapan perancangan sistem

2.2.1. Preprocessing

This pre-processing stage is a stage that aims to improve image quality, as well as sharpen the edges of the image so that image objects will be easier for the segmentation stage. The pre-processing technique used is image sharpening by implementing a kernel sharpening matrix filter, where the kernel matrix will be convolved with the raw image data obtained from the acquisition. So this process will clarify the edges of the objects in the image.

2.2.2. R-CNN Mask Model Segmentation Process

Segmentation is carried out by the Mask R-CNN model architecture. The design of the Mask R-CNN architecture uses the library from the github.com/matterport/Mask_RCNN page and the transfer learning process from larger weight training data, namely the COCO dataset [6]. To be able to carry out the segmentation process, the segmentation model first goes through a training stage and a testing stage. Each stage has its own flow diagram but is interrelated, as shown in the flow diagrams in Figure 2 and Figure 3. The training stage aims to produce a segmentation model by inputting cow object image data as well as ground truth label annotations that have been reduced in size. The training data which is divided into training data and validation data is entered into the Mask R-CNN algorithm architecture. Then, at the testing stage, the training model will be tested and evaluated for its segmentation results on test data that has been separated from the training process for the Mask R-CNN algorithm model. If the Intersection over Union

(IoU) evaluation metric exceeds 0.5 then the cow object segmentation model is acceptable and if the IoU is less than 0.5 then parameter modifications are carried out and the training stage process is repeated.

Figure 2. Flow diagram of the Mask R-CNN segmentation model training process

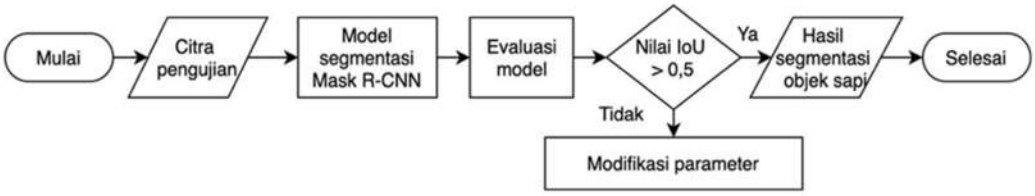

Figure 3. Flow diagram of the Mask R-CNN segmentation model testing process

2.2.3. Weight Estimation Process with CNN Regression

Weight estimation is carried out by the CNN model architecture with modification of the regression output. Regression CNN architecture design using basic architecture. This basic architecture has different image input specification characteristics as shown in Table 2 below. These four architectures implement a transfer learning process from larger weight training data, namely the ImageNet dataset. The basic architecture is then modified in the final layer by providing only one dense layer node with a linear activation function so that it resembles a linear regression process. Apart from the linear regression method, this research also implemented several methods including support vector regression (SVR) and decision tree regressor (DTR). The process of observing variations in the regression method is shown in Figure 4 below.

Table 2. Image size specifications for each CNN architecture

Arsitektur	Ukuran Citra
ResNet152V2	224 x 224
Xception	299 x 299
InceptionResNetV2	299 x 299
MobileNetV2	224 x 224

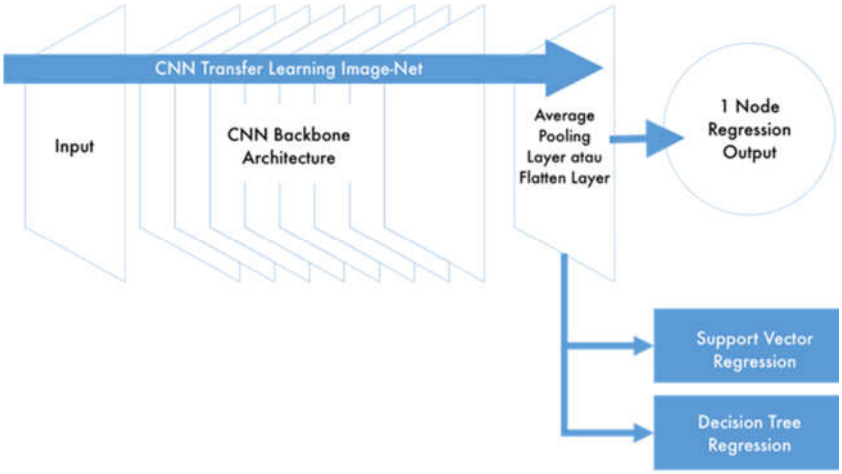

Figure 4. Illustration of the regression method variation process

After designing, so that the CNN Regression model can estimate weight, training and testing stages are carried out. Each stage has its own flow diagram but is interrelated, as shown in the flow diagrams in Figure 5 and Figure 6. The training process aims to produce a weight estimator model. Image data of cow objects

that have been segmented by the Mask R-CNN model and weight data labels in kilograms are prepared. The data is then carried out by a data augmentation process to add variation to the data, so that the data is ready to be entered into the CNN Regression algorithm architecture.

At the testing stage, the training model will be evaluated based on the difference in error or loss metrics which are calculated based on the mean squared error (MSE) metric for training data and validation data. Evaluation is carried out by looking at the difference in error between training and validation data. If the error is high, the model experiences underfitting, and when the error value for the training data is much smaller than the error value for the validation data, the model experiences overfitting. If the model does not experience these two things then the cow weight estimation model is acceptable. If the model experiences one of these things, the parameter modification process is carried out and the training process is repeated until overfitting or underfitting does not occur again.

Figure 5. Flow diagram of the CNN Regression weight estimation model training process

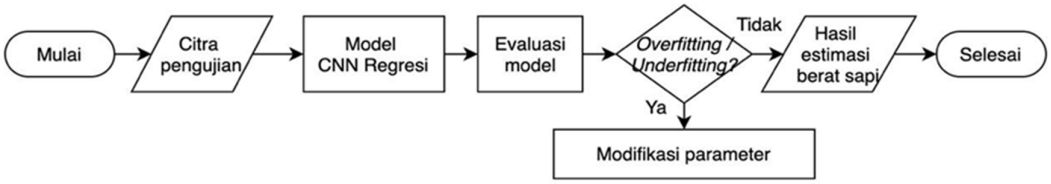

Figure 6. Flow diagram of the CNN Regression weight estimation model testing process

2.3. Evaluation of Weight Estimation Results

The system testing process is carried out on test data to determine the reliability of the system for calculating the weight estimation of cattle objects. The instruments or metrics used in measuring the performance of the weight estimator model are root mean square error (RMSE), mean absolute error (MAE), mean absolute percentage error (MAPE) and the coefficient of determination R2 metric. Below, the formula for each metric is shown in equation (1) for the RMSE metric, equation (2) for the MAE metric, equation (3) for the MAPE metric and equation (4) for the R2 metric. And it is known that this is the estimated value and yi is the actual value.

$$RMSE = \sqrt{MSE} = \sqrt{\frac{1}{N}\sum_{i=1}^{N}(y_i - \hat{y})^2} \quad (1)$$

$$MAE = \frac{1}{N}\sum_{i=1}^{N}|y_i - \hat{y}| \quad (2)$$

$$\text{MAPE} = \frac{100}{n}\sum_{i}^{n}\frac{y_i - \hat{y}_i}{y_i} \quad (3)$$

$$R^2 = 1 - \frac{\sum(y_i - \hat{y})^2}{\sum(y_i - \bar{y})^2} \quad (4)$$

3. RESULTS AND DISCUSSION

3.1. Preprocessing Results

The pre-processing stage receives input in the form of raw images resulting from data acquisition. Image data in the form of a 3 dimensional matrix is convolved with a kernel sharpening matrix. This results in a

matrix image with a higher level of sharpness. Based on the pre-processing results shown in Figure 7. The image sharpening results aim to facilitate the subsequent algorithm process in carrying out segmentation and weight estimation.

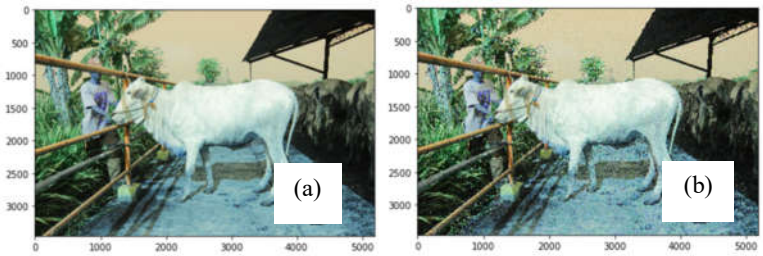

Figure 7. Data snippets of cow images (a) before sharpening (b) after sharpening

3.2. Results of the R-CNN Mask Model Segmentation Process

The segmentation process is divided into the training and testing processes of the Mask R-CNN segmentation model. Before that, an image dataset was prepared with cow object annotations in the form of a .json file. The annotation data that was collected was 150 data with a breakdown of 96 training data, 24 validation data and 30 test data. The data used in the Mask R-CNN model training process is training data and validation data which has carried out several augmentation operations including flip left-right, rotation and scale. In this training process, several metrics were observed to determine the performance of the Mask R-CNN algorithm per epoch or per unit data training process as shown in Figure 8 below.

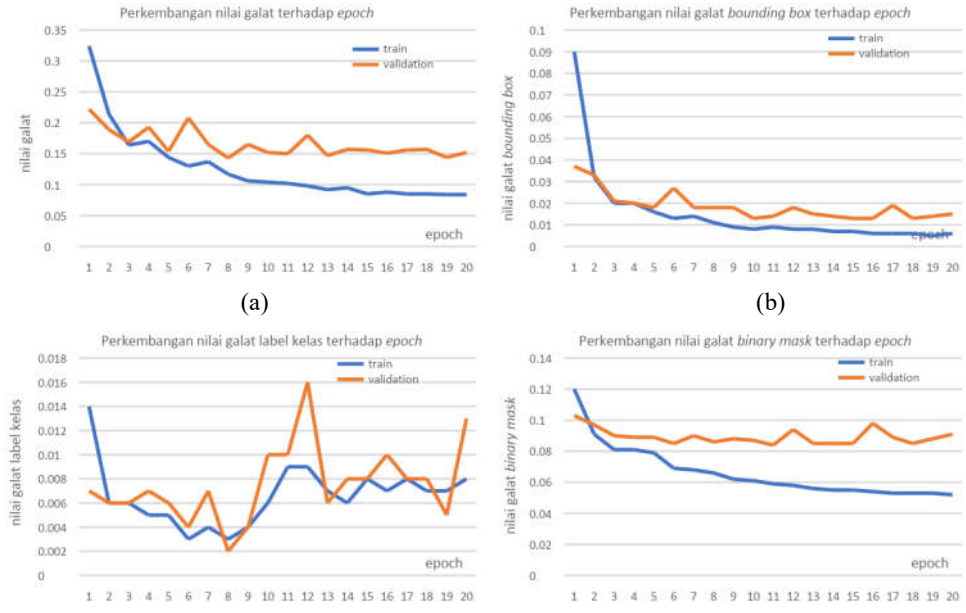

Figure 8. Graph of training results (a) error value against epoch (b) bounding box error value against epoch (c) class label error value against epoch and (d) binary mask error value against epoch

Based on the graph in Figure 8, it can be analyzed that the training process is going well because each error metric decreases as the epoch increases. However, if you pay close attention, each error value experiences an insignificant decrease in value when passing the 5th epoch and above. Even in the class label error metric the value tends to increase again. This is an indication that the training process has reached a saturation point and if it continues there is a possibility that overfitting will occur in the results of the training model. In the analysis of the calculation of the Intersectoin over Union (IoU) value, the test data as shown in the graph in Figure 9 also shows the same thing, namely that after the 6th epoch the IoU results obtained tend to fluctuate between the values of 0.85 to 0.88 so that they correlate more and more. The higher the epoch or the longer the training process, the error metric value or IoU will experience saturation. Based on the graph in

Figure 8, it can also be seen that the Mask R-CNN algorithm model in the first epoch produces very good IoU performance, this is most likely influenced by the transfer learning model from Mask R-CNN on the COCO dataset which already has a cow object class label and in one Training epochs are carried out at 1000 steps per epoch. So these two things make the initial performance of Mask R-CNN very good.

Figure 9. Graph of IoU values of test data against epoch

In addition to analysis of error metrics and IoU metrics of test data in the training process. This research also observes the influence of backbone parameter values and learning rate on the IoU metric results from test data. These results are shown in Table 3 below. Based on these results, it is known that the best influence of the learning rate value is at a value of 0.001, learning rate values below and above this value have relatively lower results. A small learning rate value (<0.001) causes the model to be too slow in correcting the weights and does not have time to reach the optimal solution from gradient descent. On the other hand, when the learning rate value is large (>0.001), it causes the model to correct the weights too much so that it passes the optimal solution point of gradient descent.

The second observation parameter is the Mask R-CNN backbone model, where the ResNet50 backbone has a smaller difference in the number of parameters and layer depth compared to the ResNet101 backbone. Based on Table 3, it is known that the more parameters and layers will increase the IoU value as seen in the learning rate of 0.0005 and 0.0001. However, this difference does not affect the IoU value for the learning rate value of 0.001 and also for the learning rate value of 0.005, the ResNet101 backbone fails to produce a segmentation model and is completely unable to segment the cow object.

Table 3. Influence of backbone parameters and learning rate on IoU values

backbone	*learning rate*			
	0,005	0,001	0,0005	0,0001
ResNet-50	0,85	0,86	0,83	0,80
ResNet-101	0	0,86	0,85	0,85

The final result of the training and testing process is a cow object segmentation model. The segmentation model is saved in the .h5 file. The following is a snapshot of the cow object segmentation results shown in Figure 10, with the highest IoU value in point (a) and the lowest point (b) in the test data.

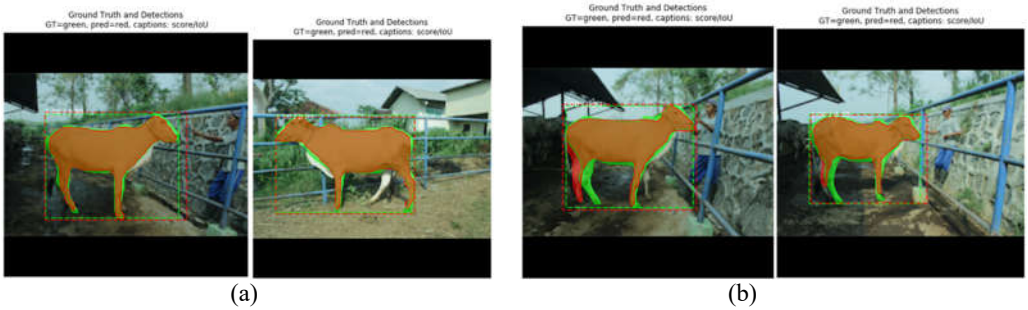

(a) (b)

Figure 10. Test data segmentation results by the Mask R-CNN model (a) the highest IoU value is 0.89 (b) the lowest IoU value is 0.77 and 0.78

3.3. Results of the CNN Regression Weight Estimation Process

Like the segmentation process, the weight estimation process is also divided into the process of training and testing the CNN Regression weight estimator model. Initial preparation was carried out by collecting a dataset of cow object images that had been segmented with cow weight data in kilograms. Several augmentation operations were carried out on the data, including a left-right flip and rotation from a tilt of -5 to 5 degrees. So that 1892 data were obtained from 86 initial data with details divided into 1209 training data, 303 validation data and 379 test data. The data used in the CNN Regression model training process is training data and validation data. The parameters used in the training process are based on similar CNN Regression research cases. In this training process, several metrics are observed to determine the performance of the CNN Regression algorithm per epoch or per unit data training process as shown in Figure 11 below.

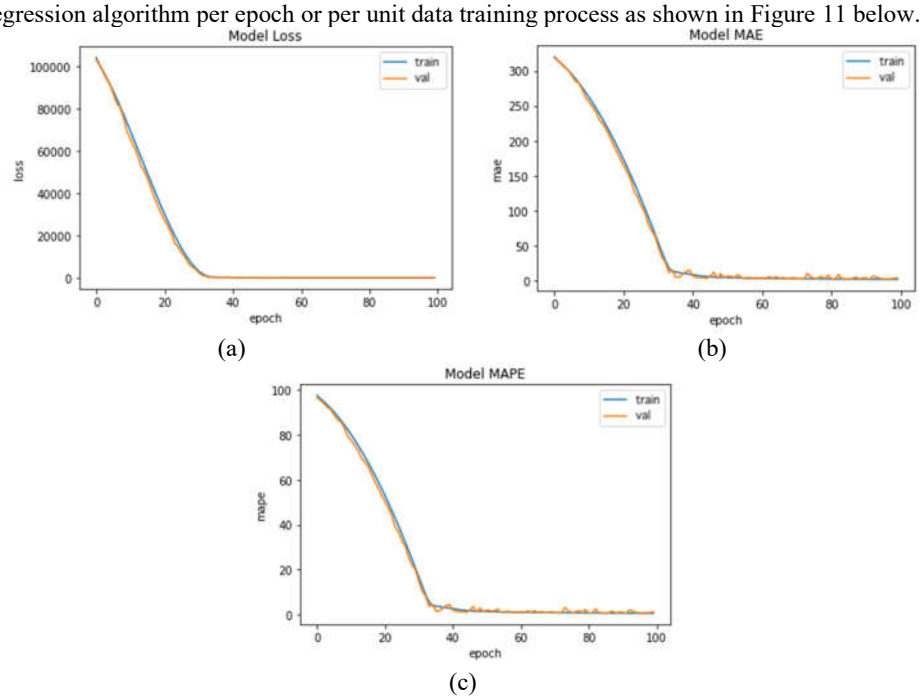

Figure 11. Graph of CNN Regression training results (a) error value or MSE against epoch (b) MAE value against epoch and (c) MAPE value against epoch

Based on the graph in Figure 11, it can be analyzed that the training process is going well because each error metric decreases as the epoch increases. Likewise, it can be seen that the model has almost the same metric values between training data and validation data. So that the model does not experience overfitting or underfitting. However, if you pay close attention, each error value experiences an insignificant decrease in value when passing the 35th epoch and above. This shows an indication that the training process has reached a saturation point.

This research observes the influence of basic CNN architecture on evaluation metrics. The results table for this influence data is shown in Table 4. Based on the data results, when viewed from the RMSE metric values, it shows that the lowest RMSE and MAE values were obtained by the Xception architecture. The RMSE metric is also used as the main benchmark because it is the standard deviation value of the weight value estimated by the model. Apart from that, the RMSE value also shows the level of difference in the volatility of the estimated results regarding the linear regression line and is more sensitive for detecting outlier data. The data on the difference between the estimated weight and the actual weight for each architectural variation is shown in the scatter plot in Figure 12 below.

Table 4. Influence of CNN architecture on evaluation metrics

Arsitektur CNN	Evaluation Metric

	RMSE	MAE	MAPE	R^2
MobileNetV2	2,70	1,96	0,61%	0,99
ResNet152V2	2,13	1,27	0,37%	0,99
Xception	1,57	1,26	0,37%	0,99
InceptionResNetV2	3,42	2,57	0,75%	0.99

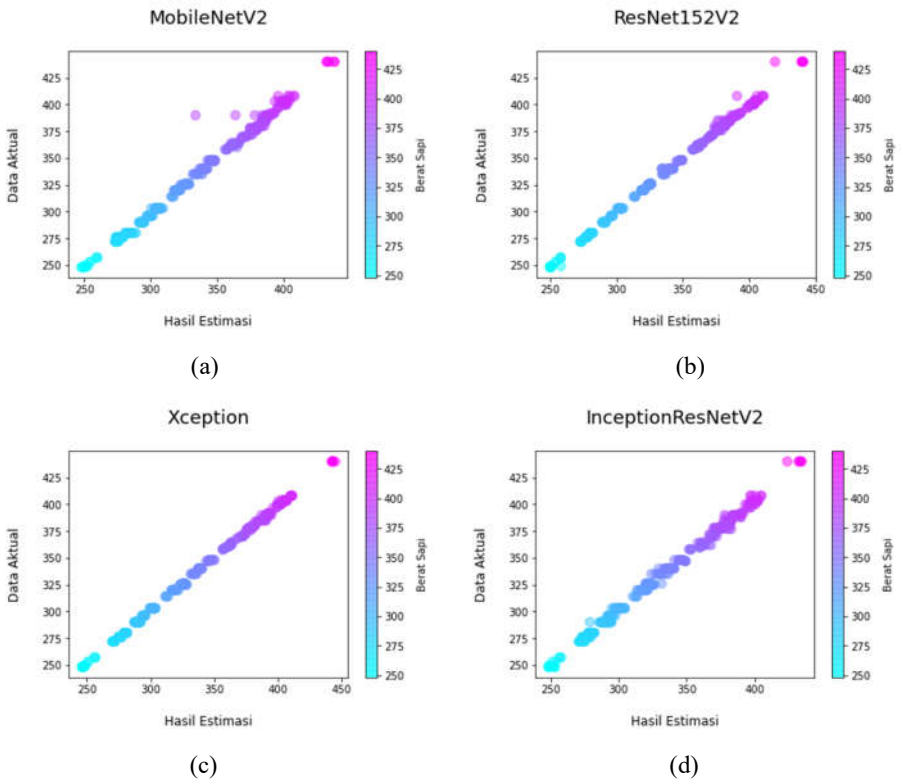

Figure 12. Comparison graph of estimated results and actual data for model (a) MobileNetV2 (b) ResNetV2 (c) Xception and (d) InceptionResNetV2

The next observation made in this research was the influence of the type of regression method. The linear regression method is a method from the previous observation process with the implementation of one node in the final CNN layer. This method was compared with other regression methods including the SVR and DTR methods by inputting the results of 2048 feature extraction data from the CNN Xception model. The parameter implementation is carried out using the default sklearn library. The results of the influence of different types of regression methods on evaluation metrics are shown in Table 5. Then the graph of the difference between the estimated weight and the actual weight for each architectural variation is shown in the scatter plot in Figure 13. Based on the results of Table 5 and the graph in Figure 13, the DTR method was successful in producing The RMSE metric value is even lower than the linear regression method, namely 1.10. Meanwhile, the SVR method actually produces higher evaluation metric results, exceeding the previous 4 variations of the CNN architecture. The scatter plot graph resulting from the SVR method also shows a different regression line with a more curved shape.

Table 5. Effect of type of regression method on evaluation metrics

Metode regresi	Metrik evaluasi			
	RMSE	MAE	MAPE	R^2

Regresi Linier	1,57	1,26	0,37%	0,99
Support Vector Regression (SVR)	5,95	2,79	0,80%	0,98
Decision Tree Regression (DTR)	1,10	0,24	0,06%	0,99

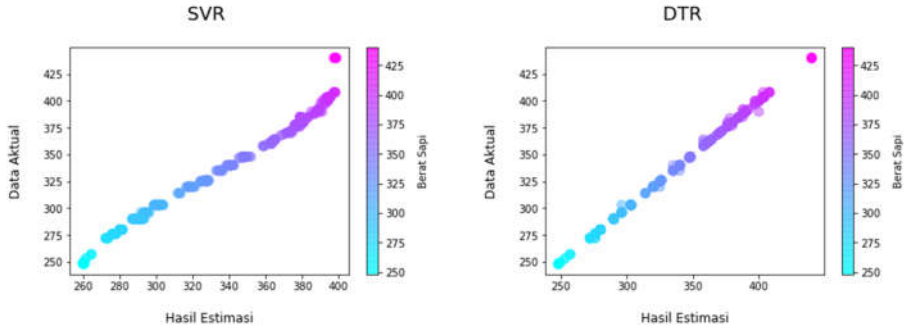

(a) (b)

Figure 13. Comparison graph of estimated results and actual data from the regression method (a) SVR and (b) DTR

The final result of the training and testing process is a cow weight estimation model. The weight estimation model is saved in the .h5 file for the CNN Xception model and .pkl for the DTR method. The following is a snapshot of the cattle weight estimation results shown in Figure 10, with the predicted values closest to point (a) and furthest to point (b) in the test data.

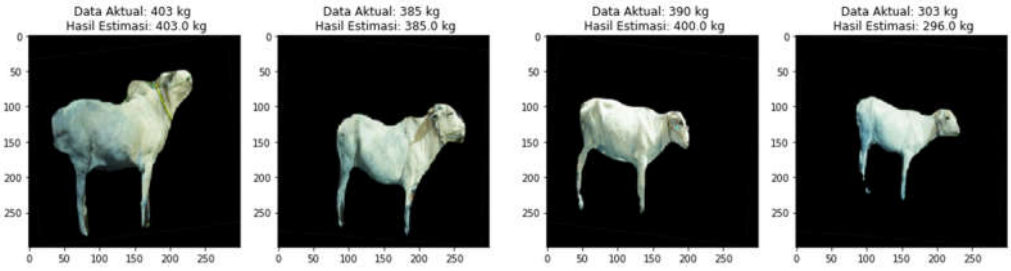

(a) (b)

Figure 14. Test data segmentation results by the CNN Regression model DTR method (a) best prediction (b) poor prediction

4. CONCLUSION

Based on the results of the system testing carried out in this research, it can be concluded that the system is able to carry out the segmentation process and estimate the weight of cattle well. In the segmentation process by the Mask R-CNN algorithm, the best test data IoU value was obtained at 0.86 with ResNet101 backbone parameters, learning rate 0.001, and epoch 5. And in the weight estimation process by the CNN Regression algorithm on the test data, the best RMSE measurement value was obtained at 1 .10. MAE 0.24. MAPE 0.06% and R2 0.99 with Xception architectural model parameters and DTR regression method.

Suggestions that can be given for further research include collecting data for other types of cattle besides ongole crossbreeds. So the system can be used more widely, not just limited to certain types of cows.

DECLARATION

Author Contribution

The material used in this research is digital image data from the side of the cow's body.

Funding

Researchers would like to thank the Kendal Class A Integrated Livestock Cultivation and Breeding Center, Central Java, which has provided data for the purposes of this research.

Acknowledgments
Researchers would like to thank the Kendal Class A Integrated Livestock Cultivation and Breeding Center, Central Java, which has provided data for the purposes of this research.

Conflict of Interest
Declare conflicts of interest or state "The authors declare no conflict of interest."

REFERENCES
[1] W. Luo, J. Sun, Y. Liao, and Z. Zhang, "Research on the Real-Time Detection Method for Image Processing – Based Civil Structure Crack," Trait. du Signal, vol. 39, no. 6, pp. 2223–2228, Dec. 2022.
[2] I. Saritas and I. Demirci, "Damage Detection of Carbon Face Sheet Nomex Sandwich Composites with Image Processing Technique," Int. J. Intell. Syst. Appl. Eng., vol. 9, no. 4, pp. 282–287, Dec. 2021.
[3] A. Eslami, M. Negnevitsky, E. Franklin, and S. Lyden, "Harmonic Source Location and Characterization Based on Permissible Current Limits by Using Deep Learning and Image Processing," Energies, vol. 15, no. 24, p. 9278, Dec. 2022.
[4] J. Fang, F. Yang, R. Tong, Q. Yu, and X. Dai, "Fault diagnosis of electric transformers based on infrared image processing and semi-supervised learning," Glob. Energy Interconnect., vol. 4, no. 6, pp. 596–607, Dec. 2021.
[5] A. Mehdi and M. Alamin, "Applying Digital Image Processing Technology in Discovering Green Patches in the Desert of Saudi Arabia," Int. J. Adv. Comput. Sci. Appl., vol. 11, no. 12, 2020.
[6] I. A. Qasmieh, H. Alquran, A. Zyout, Y. Al-Issa, W. A. Mustafa, and M. Alsalatie, "Automated Detection of Corneal Ulcer Using Combination Image Processing and Deep Learning," Diagnostics, vol. 12, no. 12, p. 3204, Dec. 2022.
[7] J. P. Martín, Y. Alvarado-Capó, R. O. Morales, T. Pichardo, and A. A. López, "Count of bacteria and yeast in microbial bioproduct using digital image processing," ITEGAM- J. Eng. Technol. Ind. Appl., vol. 7, no. 32, 2021.
[8] S. Bollmann and P. Kleinebudde, "Predictive selection rule of favourable image processing methods for X-ray micro-computed tomography images of tablets," Int. J. Pharm., vol. 610, p. 121207, Dec. 2021.
[9] L. Liu and G. Luo, "Quality Inspection Method of Agricultural Products Based on Image Processing," Trait. du Signal, vol. 39, no. 6, pp. 2033–2040, Dec. 2022.
[10] N. Hasheminejad et al., "Utilizing deep learning and advanced image processing techniques to investigate the microstructure of a waxy bitumen," Constr. Build. Mater., vol. 313, p. 125481, Dec. 2021.
[11] I. Ertugrul, "Characterization of a Micro Beam Fabricated with 3D Technology Using Image Processing Algorithm," Curr. Nanosci., vol. 16, no. 6, pp. 1024–1030, Feb. 2021.
[12] K. Schmidt, A. Trofe, and T. Ignatova, "Communication–Multimodal Image Correlation in Two-Dimensional Materials via Automated Image Processing by Strain and Doping Analysis," ECS J. Solid State Sci. Technol., vol. 11, no. 12, p. 121007, Dec. 2022.
[13] H. Wurm and M. Sandmann, "Establishment of a simple method to evaluate mixing times in a plastic bag photobioreactor using image processing based on freeware tools," BMC Res. Notes, vol. 14, no. 1, p. 470, Dec. 2021.
[14] M. Talaat, M. Tayseer, and A. El-Zein, "Digital image processing for physical basis analysis of electrical failure forecasting in XLPE power cables based on field simulation using finite-element method," IET Gener. Transm. Distrib., vol. 14, no. 26, pp. 6703–6714, Dec. 2020.
[15] T. A. Alhaj et al., "Preliminary Stages for COVID-19 Detection Using Image Processing," Diagnostics, vol. 12, no. 12, p. 3171, Dec. 2022.
[16] M. Fujitake, M. Inoue, and T. Yoshimi, "Development of an Automatic Tracking Camera System Integrating Image Processing and Machine Learning," J. Robot. Mechatronics, vol. 33, no. 6, pp. 1303–1314, Dec. 2021.
[17] J. Chen, D. Zhang, S. Yang, and Y. A. Nanehkaran, "Intelligent monitoring method of water quality based on image processing and RVFL-GMDH model," IET Image Process., vol. 14, no. 17, pp. 4646–4656, Dec. 2020.

[18] W. Tan, P. Ren, Y. Wang, Y. Wang, and G. Zhu, "Experimental Study on Fluidelastic Instability of Tube Bundles With Asymmetric Stiffness Using Visual Image Processing System," J. Press. Vessel Technol., vol. 144, no. 6, Dec. 2022.
[19] Z. Li, X. Han, L. Wang, T. Zhu, and F. Yuan, "Feature Extraction and Image Retrieval of Landscape Images Based on Image Processing," Trait. du Signal, vol. 37, no. 6, pp. 1009–1018, Dec. 2020.
[20] F. Matsui, F. Watanabe, T. Nakamura, and M. Yamaguchi, "Unmixing of the background components in an off-axis holographic-mirror-based imaging system using spectral image processing," Opt. Express, vol. 28, no. 26, p. 39998, Dec. 2020.
[21] P. M. Prasuna, Y. Ramadevi, and A. V. Babu, "A Distributed Environment with Rough Set Theory Based Image Processing Approach for Analysis of Facial Disorders for Better Cosmetic Product Recommendation," Int. J. Saf. Secur. Eng., vol. 10, no. 6, pp. 777–784, Dec. 2020.
[22] J. Michelet, M. M. Tekitek, and M. Berthier, "Multiple relaxation time lattice Boltzmann schemes for advection-diffusion equations with application to radar image processing," J. Comput. Phys., vol. 471, p. 111612, Dec. 2022.
[23] W. Jasim and R. Mohammed, "A Survey on Segmentation Techniques for Image Processing," Iraqi J. Electr. Electron. Eng., vol. 17, no. 2, pp. 73–93, Dec. 2021.
[24] M. Weitzel, S. K. Mitra, M. Szakáll, J. P. Fugal, and S. Borrmann, "Application of holography and automated image processing for laboratory experiments on mass and fall speed of small cloud ice crystals," Atmos. Chem. Phys., vol. 20, no. 23, pp. 14889–14901, Dec. 2020.
[25] W. Cui, R.-C. Miao, W.-S. Yan, H. Song, and Z. Jiang, "Static segregation of fresh high workable concrete based on an image processing method," Constr. Build. Mater., vol. 361, p. 129708, Dec. 2022.
[26] V. G. Bondur, T. N. Chimitdorzhiev, A. V. Dmitriev, and P. N. Dagurov, "Methods of Radar Interferometry and Optical Satellite Image Processing to Study Negative Effects on the Environment (a Case Study of the Baikalsk Pulp and Paper Mill)," Izv. Atmos. Ocean. Phys., vol. 57, no. 12, pp. 1527–1537, Dec. 2021.
[27] O. Hassanijalilian, C. Igathinathane, S. Bajwa, and J. Nowatzki, "Rating Iron Deficiency in Soybean Using Image Processing and Decision-Tree Based Models," Remote Sens., vol. 12, no. 24, p. 4143, Dec. 2020.
[28] N. N. Hung, C. H. Tinh, and D. V. Minh, "Real-Time Implementation of a Novel Automatic Gain Control Algorithm for Infrared Image Processing Based on MPSoC," Autom. Control Comput. Sci., vol. 56, no. 6, pp. 577–586, Dec. 2022.
[29] M. Koklu, M. Altin, and Y. S. Taspinar, "Fire Detection inImages Using FrameworkBased on Image Processing, Motion Detection and Convolutional Neural Network," Int. J. Intell. Syst. Appl. Eng., vol. 9, no. 4, pp. 171–177, Dec. 2021.
[30] S. Jung, "Image Processor and RISC MCU Embedded Single Chip Fingerprint Sensor," J. Sens. Actuator Networks, vol. 9, no. 4, p. 51, Nov. 2020.